A cortical potential reflecting cardiac function

Marcus A. Gray*[†], Peter Taggart[‡], Peter M. Sutton[‡], David Groves[§], Diana R. Holdright[¶], David Bradbury*, David Brull[‖], and Hugo D. Critchley*[,**]

*Functional Imaging Laboratory, Wellcome Department of Imaging Neuroscience, Institute of Neurology, University College London, 12 Queen Square, London WC1N 3BG, United Kingdom; [‡]The Hatter Cardiovascular Institute, Division of Medicine, Royal Free and University College Medical School, 67 Chenies Mews, London WC1E 6HX, United Kingdom; [§]National Refractory Angina Centre, Royal Liverpool and Broadgreen University Hospital, NHS Trust, Thomas Drive, Liverpool L14 3PE, United Kingdom; [¶]The Heart Hospital, University College London Hospitals, 16–18 Westmoreland Street, London W1G 8PH, United Kingdom; [‖]The Whittington Hospital, NHS Trust Hospitals, Highgate Hill, London N19 5NF, United Kingdom; and **Department of Psychiatry, Brighton and Sussex Medical School, University of Sussex, Falmer, Brighton BN1 6PX, United Kingdom

Emotional trauma and psychological stress can precipitate cardiac arrhythmia and sudden death through arrhythmogenic effects of efferent sympathetic drive. Patients with preexisting heart disease are particularly at risk. Moreover, generation of proarrhythmic activity patterns within cerebral autonomic centers may be amplified by afferent feedback from a dysfunctional myocardium. An electrocortical potential reflecting afferent cardiac information has been described, reflecting individual differences in interoceptive sensitivity (awareness of one's own heartbeats). To inform our understanding of mechanisms underlying arrhythmogenesis, we extended this approach, identifying electrocortical potentials corresponding to the cortical expression of afferent information about the integrity of myocardial function during stress. We measured changes in cardiac response simultaneously with electroencephalography in patients with established ventricular dysfunction. Experimentally induced mental stress enhanced cardiovascular indices of sympathetic activity (systolic blood pressure, heart rate, ventricular ejection fraction, and skin conductance) across all patients. However, the functional response of the myocardium varied; some patients increased, whereas others decreased, cardiac output during stress. Across patients, heartbeat-evoked potential amplitude at left temporal and lateral frontal electrode locations correlated with stress-induced changes in cardiac output, consistent with an afferent cortical representation of myocardial function during stress. Moreover, the amplitude of the heartbeat-evoked potential in the left temporal region reflected the proarrhythmic status of the heart (inhomogeneity of left ventricular repolarization). These observations delineate a cortical representation of cardiac function predictive of proarrhythmic abnormalities in cardiac repolarization. Our findings highlight the dynamic interaction of heart and brain in stress-induced cardiovascular morbidity.

afferent homeostatic feedback | electroencephalography | heart beat-evoked potential | insula cortex | ischemia

Emotional events and mental stress can precipitate cardiac arrhythmia and sudden death in patients with heart disease (1–4). Electrocardiographic (ECG) indices of proarrhythmic electrical instability of the myocardium accompany psychological stress (5) and are associated with abnormalities in regional brain activity, suggesting abnormal efferent autonomic drive to the heart (1, 6). Although a central efferent mechanism for arrhythmogenesis may also explain sudden death in disorders such as epilepsy (4, 7), disturbances in cardiac afferent feedback may induce cardiogenic reflexes that enhance the vulnerability of cardiovascular disease patients to stress-induced arrhythmia (8). Abnormalities in wall motion and compromised myocardial function are likely to be amplified during stress-induced arousal states, resulting in perturbation of cardiac afferent information. Afferent feedback information from the heart guides efferent autonomic cardiovascular control (9, 10). By extension, abnormalities in afferent cardiac feedback can enhance arrhythmic risk (11).

Neurophysiological studies in animals of afferent representations of the heart focus primarily on projections to brainstem nuclei. Attempts to localize cardiac afferent representations in humans using functional brain imaging (6, 12–16) are constrained by the temporal resolution of the techniques. Nevertheless, such studies confirm a hierarchy of representations of cardiac function from brainstem to cortex, to a level where conscious awareness of heart function is associated with enhanced activity within anterior cingulate and insula cortices (12–14). Electroencephalography (EEG) has higher temporal resolution than techniques such as positron emission tomography or functional MRI (fMRI), although is limited with respect to inferring neuroanatomical generators of surface potentials. EEG methods have been applied to the study of afferent cardiac signals, where a heartbeat-evoked potential (HEP) has been described (17–20). The circumscribed location of this HEP to frontal and central scalp (17, 18, 21, 22) and particularly the observation that its amplitude predicts individual differences in interoceptive awareness (accuracy of heartbeat perception) (19) is consistent with a cardiac afferent source, arising from myocardial, carotid sinus and/or aortic arch baroreceptors, or perhaps mechanoreceptors within tissue distended by ejected blood (23–25). The association between HEP and pro-arrhythmic cardiac function however has not to date been investigated.

Mental stress can induce proarrhythmic electrocardiological changes and compromise ventricular function in vulnerable patients (2, 5, 6, 26). The brain correlates of this effect, mediated through stress-induced autonomic drive to the heart (increased sympathetic tone and decreased parasympathetic tone), was examined in a positron emission tomography (PET) study of cardiovascular patients. A stress-induced lateralized of brainstem activity was observed to be associated with pro-arrhythmic changes in ECG (5). Further, cortical regions including bilateral insula, anterior cingulate and orbitofrontal cortices have been shown to be modulated by baroreceptor activation (16, 27, 28). Higher temporal-resolution EEG methods overcome the timing constraints of PET or functional MRI studies and can be applied to identify cortical responses arising from cardiac afferent feedback during the cardiac cycle, i.e., HEPs generated with each heartbeat. The present study extends this EEG research to establish an index of cardiac afferent information that specifically reflects myocardial function and dysfunction during induced stress. This research is relevant to understand cardiac mortality, because abnormal afferent feedback signals may drive proarrhythmic autonomic effects on the heart, most likely interacting at the level of the brainstem (6). This afferent signal of abnormalities in myocardial function would also be rerepresented in the cortex and apparent in the distribution and amplitude of a

Fig. 1. Stress-induced changes in physiological variables. Mental stress induced by serial subtraction task was associated with significant increases in systolic blood pressure, heart rate, and ejection fraction. Mean changes in physiological parameters across all subjects are presented.

HEP. We therefore examined cardiological patients during states of enhanced sympathetic cardiovascular arousal induced using a pressor task (mental stress; serial seven subtraction). We anticipated a spectrum of functional myocardial responses across patients. In particular, we anticipated that stress challenge would evoke changes in cardiac output, heart wall motion, and electrophysiological homogeneity, in accordance with the nature and extent of cardiac pathology, and that cortical HEPs would: (*i*) reflect afferent cardiac information (i.e., myocardial response rather than generalized indices of sympathetic arousal), (*ii*) predict functional impairment in these cardiovascular patients, and (*iii*) predict proarrhythmic ECG changes in response to stress.

Results

Physiological and Cardiological Measures. Across patients, mental stress was associated with enhanced cardiovascular and electrodermal measures of sympathetic arousal. Mental stress evoked significant increases in skin conductance level (SCL) [$F(1,6) = 9.853, P = 0.020$], systolic [$F(1,9) = 46.774, P = 0.000$] and diastolic blood pressure [$F(1,9) = 48.027 P = 0.000$], ejection fraction [$F(1,9) = 8.631, P = 0.017$], and heart rate [interbeat interval $F(1,9) = 6.673, P = 0.030$] (Fig. 1).

ECG Changes. Consistent with proarrhythmic effects on repolarization, mental stress was associated with significantly increased inhomogeneity of repolarization (Hill parameter lead V3) [$t(8) = 3.493, P = 0.010$]. Further, mental stress was associated with significantly increased T-wave amplitude {lead F [$t(6) = 3.479, P = 0.013$], lead V3 [$t(8) = 2.411, P = 0.042$] and lead V4 [$t(8) = 3.023, P = 0.016$]}. Importantly, because stress was associated with significant ECG T-wave alterations, we selected our HEP epoch during the period following the T wave (Fig. 2). Repeated-measures analysis of ECG recorded at the neck revealed no significant difference in mean ECG amplitudes (455–595 ms after R wave) between the baseline and stress-task conditions.

Main Effect of Stress on HEP. We observed no overall alteration across electrodes in the amplitude of HEP (455–595 ms after R wave) as a function of mental stress (*t* tests of change in HEP, stress-baseline, 2D scalp space; Fig. 3). This result is a noteworthy indication that the changes in HEP described below do not have a primary relationship to cognitive processing and mental effort. Nevertheless, significant correlations were observed across individuals between HEP amplitude and the functional myocardial response to the mental stress challenge. These are detailed below.

HEP as Index of Cardiac Output. Two circumscribed clusters of significant association between HEP and cardiac output change (independent of changes in systolic blood pressure) were observed in left temporal and lateral frontal regions. These clusters retained significance after correction for multiple comparisons (*P* value correction on spatial extent of individual electrode associations significant at $P < 0.001$; cluster level correction $P = 0.001$) and are
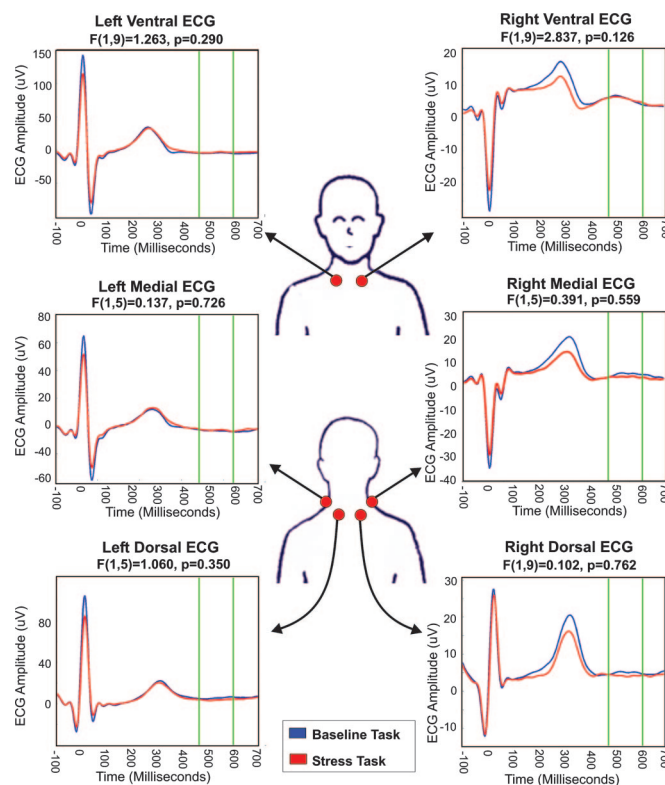
Fig. 2. ECG amplitude during baseline and stress task conditions. ECG was measured at six locations around the base of the neck. No significant differences in ECG amplitude were observed during the post-T-wave epoch (140 ms average from 455 to 595 ms after R wave).

shown in Fig. 4*A*). Within each region, individual pair-wise correlations reveal that increased cardiac output was associated with increased HEP negativity. This is illustrated in Fig. 4*B* with peak electrodes from each significant cluster. In summary, the HEP at left temporal and lateral frontal surface electrodes specifically reflected individual patient differences in the magnitude of evoked myocardial response to stress. Examination of multivariate interaction of hemisphere (left HEP/right HEP) with the covariate cardiac output revealed a significant interaction [$F(1,5) = 6.225, 0.037$]. This interaction demonstrates a hemispheric effect, that is, a significantly greater HEP cardiac output association within the previously identified left temporal cluster than within the corresponding region of the right hemisphere [see supporting information (SI)].

Association Between Changes in Cardiac Repolarization Homogeneity and HEP. Changes in the cardiac repolarization [indexed by the Hill parameter; see *Materials and Methods*] were also significantly associated with HEP changes in the left temporal region (individual electrode correlations significant at $P < 0.002$; cluster level correction $P = 0.032$; Fig. 5*A*). Increases in inhomogeneity of cardiac repolarization were associated with increases in the negative amplitude of the HEP in this region (Fig. 5*B*). Again, a multivariate interaction of hemisphere (left HEP/right HEP) with the covariate Hill parameter demonstrated a significantly greater association within the left temporal cortex than within the corresponding region of the right hemisphere [$F(1,5) = 10.922, P = 0.021$].
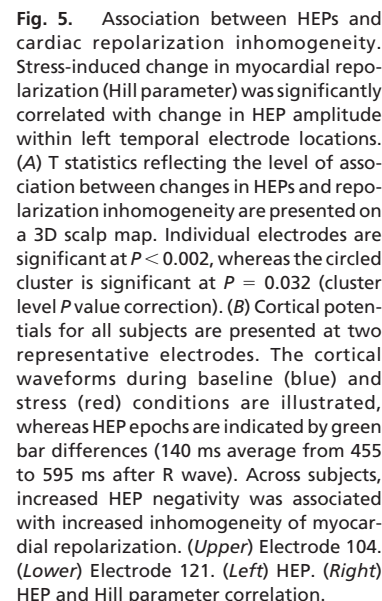
Importantly, there was no significant linear association between T-wave amplitude or heart rate change and changes in HEPs or between cardiac output and cardiac repolarization.

Discussion

We report a brain potential, maximal at left temporal and lateral prefrontal surface electrodes, which reflects afferent neural infor-

Fig. 3. HEPs during stress and baseline conditions. Mental stress was not associated with significant alteration in HEP amplitude. (*A*) HEPs at all scalp locations are shown for both the baseline (blue) and mental stress (red) conditions. In all graphs, up represents positive ERP deflections. (*B*) HEPs at standard 10/20 international electrode placement system positions are enlarged. In addition, HEP epochs (140 ms centered at 525 ms after R wave) are highlighted by green bars. (*Left*) Left hemisphere electrodes. (*Right*) Right hemisphere electrodes. (*C*) Average ERP difference waveforms displayed in 2D scalp space. Across subjects, no significant alterations in HEPs were observed during mental stress. Greater negative HEPs during the high-stress condition are illustrated toward the blue end of the spectrum, whereas greater positive HEPs during the high-stress condition are shown toward the red end of the spectrum.

mation from myocardium. This HEP occurs after each heartbeat, correlates with functional and dysfunctional cardiac responses in cardiovascular patients, and has a predictive relationship with respect to proarrhythmic changes in electrical repolarization of the heart in response to stress, as reflected in correlations with the Hill parameter.

Our work is predicated on studies describing afferent "interoceptive" potentials triggered on the heart (17–20, 29). However, in contrast to previous findings, our research represents a demonstration of cortically recorded indices of cardiac function in a clinical population. Consistent with the induction of mental stress, performance of the serial subtraction task increased sympathetic drive to the heart and periphery (reflected directly by increased skin conductance heart rate and systolic and diastolic blood pressure). Nevertheless, we did not observe, across patients, a consistent increase in cardiac output as a consequence of increased sympathetic drive to the heart. Rather, although five patients showed hypereffective cardiac responses, within the remaining patients cardiac output fell. The left temporal/lateral frontal HEP mirrored these functional responses of the myocardium where greater cardiac output (independent of peripheral measures such as systolic pressure) was associated with greater HEP negative amplitude.

The normal physiological response of the heart to enhanced sympathetic drive is to alter force–tension–velocity relations to increase effective performance. The concomitant increases in stroke volume and cardiac output impact on systolic blood pressure (largely regulated peripherally). However, patients with compromised ventricular function can show a reduction in cardiac output during increased sympathetic drive. This may result from a failure of the impaired myocardium to increase cardiac output by increasing effective myocardial contraction in the face of increasing metabolic demand and the action of cardio-cardiac reflexes. All patients in our study had evidence of ventricular wall abnormality, with either regions of infarcted myocardium, echocardiographic evidence of impaired contractile function, or both (Table 1) accounting for the mixed hemodynamic profile we observed during stress. The diversity in observed HEP amplitude corresponded to diversity in myocardial function (cardiac output) rather than general indices of sympathetic activity, consistent with the notion that HEP is tuned to cardiac afferent feedback representation rather than efferent cardiac control. Similar considerations apply to measures of inhomogeneity of myocardial repolarization, with some patients showing an increase in inhomogeneity of repolarization during stress, whereas others showed decreased inhomogeneity. Both stretch and altered length of fiber excursion influence

Fig. 4. Association between HEPs and cardiac output. Stress-induced change in cardiac output was significantly correlated with change in HEP amplitude within left temporal and posterior frontal electrode locations. (*A*) T statistics reflecting the level of association between changes in HEPs and cardiac output are presented on a 3D scalp map. Individual electrodes are significant at $P < 0.001$. Each circled cluster is also significant at $P = 0.001$ (cluster level P value correction). (*B*) Cortical potentials for all subjects are presented at a representative electrode from within each significant cluster. The cortical waveforms during baseline (blue) and stress (red) conditions are illustrated, whereas HEP epochs are indicated by green bar differences (140 ms average from 455 to 595 ms after R wave). Across subjects, increased HEP negativity was associated with increased cardiac output during stress. (*Upper*) Electrode 100. (*Lower*) Electrode 118. (*Left*) HEP. (*Right*) HEP and cardiac output correlation.

Fig. 5. Association between HEPs and cardiac repolarization inhomogeneity. Stress-induced change in myocardial repolarization (Hill parameter) was significantly correlated with change in HEP amplitude within left temporal electrode locations. (*A*) T statistics reflecting the level of association between changes in HEPs and repolarization inhomogeneity are presented on a 3D scalp map. Individual electrodes are significant at $P < 0.002$, whereas the circled cluster is significant at $P = 0.032$ (cluster level P value correction). (*B*) Cortical potentials for all subjects are presented at two representative electrodes. The cortical waveforms during baseline (blue) and stress (red) conditions are illustrated, whereas HEP epochs are indicated by green bar differences (140 ms average from 455 to 595 ms after R wave). Across subjects, increased HEP negativity was associated with increased inhomogeneity of myocardial repolarization. (*Upper*) Electrode 104. (*Lower*) Electrode 121. (*Left*) HEP. (*Right*) HEP and Hill parameter correlation.

action potential duration through mechanoelectric feedback by effecting sarcolemmal stretch-activated channels and intracellular calcium cycling (26). Among our patients, the effects of stress on the homogeneity of myocardial repolarization varied, some patients increasing and others decreasing the evenness of myocardial repolarization. Once again, the diversity of HEP amplitude was more closely related to diversity in the myocardial repolarization than with increases in sympathetic activity, i.e., consistent with cardiac afferent feedback rather than efferent cardiac drive.

A prominent source of cardiac afferent signal arises from low threshold baroreceptors and mechanoreceptors of the ventricular myocardium, carotid sinus, and aortic arch. These respond to stretch, compression, and deformation, thereby signaling information about cardiac filling and function. This information is conveyed centrally along vagus nerve and spinal afferents to influence centrally mediated cardio-cardiac reflexes (30, 31). Stimulation of vagus nerve afferents may decrease myocardial contractility, stroke volume, and cardiac output through reflex withdrawal of sympathetic neural tone. In contrast, stimulation of sympathetic afferents can induce the opposite effects principally by increasing sympathetic efferent activity but also through parasympathetic withdrawal. An important feature of baroreceptor-mediated information is that it occurs in a cyclical fashion in time with the cardiac cycle. Baroreceptor activation underlies repeated inhibition of muscle sympathetic nerve activity occurring during each cardiac

cycle (32). Importantly, cardiac output provides a superior between-subject index of baroreceptor activation, which may be independent of systolic blood pressure differences (33). Our findings extend neuroimaging observations of central baroreflex responses (16, 27) to show a direct modulation of cortical activity by afferent baroreceptor information within each cardiac cycle.

Human and animal studies suggest this cardiac afferent information is relayed hierarchically through the CNS by nucleus of the solitary tract, medulla, parabrachial nucleus, hypothalamus, and thalamus (34–36). It is at these brainstem and subcortical levels that central cardio-cardiac reflexes may exacerbate pathological autonomic responses to emotional challenges in cardiological patients placing them at risk of arrhythmia and sudden death (1, 6, 9). Beyond these brainstem centers, homoeostatic afferent information is conveyed by both basal and posterior ventromedial thalamic nuclei to the superior margin of the insula cortex, which supports a cortical representation of visceral state (9, 34, 37–42). Mid- and posterior insula regions appear to map physiological afferent information in an anatomically graded somatotopic mapping of the viscera (38, 43, 44). Rerepresentation of this afferent information by anterior insula regions is implicated as the substrate for awareness and conscious appraisal of physiological status where information about internal state is integrated with ongoing emotional processing (19, 38, 40–42). Correspondingly, in patients with cardiac syndrome X, dobutamine-induced cardiac afferent sensation

Table 1. Patient clinical profiles

Patient	Age	Sex	MI	Wall mot	Current medications		
					β-blk	Ca-blk	ACE
1	63	M	No	Mod	No	Diltiazem	Ramipril
2	60	M	Yes	Mod	Atenolol	No	Ramipril
3	55	M	Yes	Mild	Atenolol	Diltiazem	Ramipril
4	60	M	Yes	Mod	Atenolol	No	No
5	45	M	Yes	Mod	Atenolol	No	Ramipril
6	77	M	Yes	Mild	Atenolol	Diltiazem	Lisinopril
7	58	M	Uncertain	Mild	Atenolol	No	No
8	42	M	Yes	Mod	Bisoprolol	No	Perindopril
9	71	M	Dilated	Severe	Bisoprolol	No	No
10	58	M	Yes	Severe	Atenolol	Amlodipine	Perindopril

One patient had one-vessel heart disease, with all remaining patients having two-to-three vessel heart disease. In addition, patients 2 and 8 had undergone coronary artery surgical procedures; patients 7 and 10 had undergone angioplasty procedures; and patients 2, 9, and 10 had previous heart failure. MI, myocardial infarction; Wall mot, ventricular wall motion impairment; β-blk, beta blocker; Ca-blk, calcium channel blocker; ACE, angiotensin-converting enzyme inhibitor. M, male.

NEUROSCIENCE

(angina) pain is associated with enhanced insula cortex activity (45, 46). Right-sided afferent representations within anterior insula are linked to conscious interoceptive processing. However, studies of rodents and non-human primates clearly demonstrate direct representations of baroreceptor activity within bilateral insular cortex (24, 47, 48). Our findings associate left hemisphere activity with largely unconscious alterations in myocardial function. Together, these observations highlight the role of insula in supporting afferent cortical representations of cardiac function. In the present study, we describe a surface potential that relates to afferent cardiac function and adaptive cardiac response to stress. Although we are cautious in ascribing a precise neuroanatomical origin to this HEP, its location on left temporal surface electrodes suggests a neural representation within insular cortices, in accordance with other studies. An alternative interpretation of HEP changes during mental stress is that they reflect "central command" processes controlling myocardial function. Cardiac efferent responses including tachycardia, bradycardia (49–51), and the induction of lethal arrhythmias (52) have been demonstrated after insular cortex stimulation, consistent with centralized cardiac efferent control (53, 54). Although it is also possible that alterations in HEPs reflect sympathetic outflow underlying cardiac output, independent of sympathetically mediated increases in skin conductance, blood pressure, and heart rate (55), considering that cardiac output may directly index baroreceptor activation on a beat-by-beat basis, and the specific expression of our effects within each cardiac cycle, we favor an afferent representation interpretation. Further, conduction velocity research in humans indicates that baroreceptor afferents are processed centrally 400–800 ms after ECG R wave (56), consistent with HEP effects observed 450–695 ms after R wave.

In addition to cardiac output, the degree of left temporal HEP change during mental stress was directly associated with increases in myocardial repolarization inhomogeneity. This is consistent with previous findings among patients with compromised myocardial function of both increased action potential duration (APD) during adrenalin administration and increased T-wave measures of repolarization inhomogeneity during mental stress. Together, these observations illustrate that sympathetic arousal contributes to proarrhythmic changes affecting the myocardium (5, 57). During stress, enhanced sympathetic stimulation alters repolarization and APD (by influencing calcium and potassium currents) decreasing the recovery time of the myocardium. In pathological hearts with regions of infarction and wall motion abnormality, the electrophysiological effects of stretch depend on the prevailing contractile geometry. As a consequence, mechanoelectric feedback signals are themselves inhomogeneous. Moreover, uneven wall motion may potentate mechanoreceptor activation within the myocardium, increasing cardiac afferent output (observed in our study as an increase in the negative amplitude of the left temporal HEP). We are only beginning to unravel the nature and contribution of central mechanisms in determining cardiac response and risk. Nevertheless, the present study identifies a surface brain potential that indexes afferent information about myocardial function and reflects a measure of the clinical risk of stress-induced cardiac events in a vulnerable patient group.

These findings report cortical representation of cardiac afferent information reflecting myocardial response to mental stress. Within this patient sample, mental stress was associated with both increased sympathetic drive and myocardial responses ranging from hypo- to hypereffective changes in cardiac output. These functional changes were associated with changes in the amplitude of a localized HEP. Hypereffective responses were associated with increased HEP negativity within the left temporal region, consistent with a cortical rerepresentation of baroreceptor-mediated cardiac afferent information. The correlation between cardiac repolarization and HEP amplitude links myoelectrical dysfunction of the heart with changes in afferent brain response, providing insight into central feedback mechanisms that potentiate arrhythmogenesis in vulnerable cardiological patients during stress or emotional challenge.

Materials and Methods

Participants. Ten male subjects (mean age 59 yrs, $\pm$ SD = 11.11 yrs) were recruited consecutively from two cardiology outpatient clinics (The Heart Hospital, University College London Hospitals Trust, London, U.K., and The Whittington Hospital, Hampstead, London, U.K.). All had a previous history of cardiac dysfunction and were receiving pharmacological treatment (Table 1). The study was approved by the local Ethics Committee. Each patient was provided with detailed information regarding the study before giving informed consent.

Task and Design. We used a validated mental stress/pressor task (serial seven subtraction task). This task is routinely used in autonomic function testing and commonly provokes changes in cardiac and vascular function after increased sympathetic arousal. During this task, patients were required to rapidly count backward by sevens and were repeatedly encouraged to hurry while any errors were explicitly noted and corrected. This high-stress condition was contrasted with a low-stress or baseline condition, during which patients were simply required to count aloud from 1 to 50 in a regular and relaxed fashion.

Procedure. Patients were fitted with an ambulatory 12-lead ECG recorder (Del Mar Reynolds, Hertford, U.K.) monitor (standard electrode positions) and headcap containing 128 EEG electrodes before being seated in a quiet temperature-controlled electrically shielded testing room. An inflatable finger cuff and infrared plethysmograph were fitted to the index finger of the patient's right hand, allowing measurements of beat-to-beat finger arterial blood pressure with a Finometer (Finapress Medical Systems, BV, Amsterdam, The Netherlands). Electrodes for recording electrodermal activity were also applied to the distal phalanx of the first and third fingers of each hand, allowing bilateral recording of skin conductance level using AT64SCR (Autogenic Systems, Wood Dale, IL) equipment simultaneous with electrocortical and cardiac data. Subjects completed 10 min of the baseline and high-stress task conditions while seated in a semirecumbent position, with each condition split into two 5-min blocks to minimize habituation during the high-stress condition.

EEG Recording. EEG was recorded with a 128-lead sintered Ag-AgCl electrode Biosemi (Biosemi, Amsterdam, The Netherlands) Active Two system with two additional ear and six additional ECG electrodes applied using Parker Signal gel (Parker Laboratories, Fairfield, NJ). Analogue voltages, amplified at each electrode site with a recording bandwidth (-3 dB) between DC-134 Hz, were sampled at 512 Hz. Electrode-offset voltages were kept below 50 mV throughout the recording. All channels were referenced to linked ears before offline storage. Preprocessing began with band-pass filtering (0.7–24 Hz) and down-sampling to 300 Hz using statistical parametric mapping (SPM). Independent component analysis was then performed on continuous EEG data using EEGLAB (EEGLAB 4.515, University of San Diego, San Diego, CA) separately for each recording block for each subject. Eye movements and blink artifacts were removed by subtracting independent components reflecting these artifacts (58). In addition to 128 channels of EEG, ECG was recorded at the left and right collarbone within all subjects for identification of PQRS-T complexes and subsequent segmentation of EEG. Because ECG T-wave expression varies depending on the combination of ECG leads examined, we also recorded ECG at lateral and dorsal sites at the base of the neck within six subjects, allowing a comprehensive identification of T-wave expression (Fig. 2). These ECG measures were recorded as extra EEG channel data, referenced to linked ear electrodes, and preprocessed in an identical manner to EEG data. PQRS-T complexes in additional ECG leads were then identified

in Matlab (Mathworks, Billerica, MA) using custom-written software, allowing 800-ms epochs (100 ms before ECG R wave to 700 ms after ECG R wave) (17) to be selected in SPM5. EEG dud electrodes were removed from averaged HEPs for each task condition and replaced with the average of four surrounding electrodes. Difference waveforms reflecting stress associated change in HEPs were then calculated by subtracting the average baseline HEPs from the average mental stress HEPs for each subject.

Electrocardiography. The shape and distribution of ST- and T-wave segments of the 12-lead ECG provide information on the homogeneity of cardiac electrical repolarization and, in view of the prime importance of inhomogeneity of repolarization in arrhythmogenesis, were a focus of interest in the present study. Using paired t tests, we examined T-wave amplitude and accumulated T-wave area, extending from the ECG J point to the next P wave (59). Applying the Hill equation (a mathematical function parameterizing sigmoidal enzyme kinetic myocardial reactions) to measures of accumulated T-wave area provides a validated and sensitive index of ventricular repolarization inhomogeneity (60).

Physiological Measures. Beat-to-beat reconstructed brachial pressure waveforms were calculated from the finger arterial pressure waveform recorded on the Finometer. A range of physiological measures was derived from these waveforms using Beatscope software (Beatscope 1.1a, Finapress Medical Systems, BV), including brachial pressure at systole and diastole, stroke volume, interbeat interval, cardiac output, left ventricular ejection time, diastolic pressure time index (DPTI), and the maximal steepness of the upstroke [delta pressure/delta time (dp/dt)]. Skin conductance level data for each hand were derived from bilaterally recorded electrodermal activity. All of the physiological measures were averaged within the baseline and mental stress conditions separately for each patient, after which difference scores were calculated as with EEG data.

EEG Analysis. EEG measures of heart-related potentials are made more difficult by the superimposition of ECG waveform, generated within the myocardium, across scalp electrodes. Examining the influence of cardiac field artifacts (CFA) (21, 23) reported that, after the ECG T wave (350–650 ms after R wave within these subjects), ECG amplitude dropped to <1% of total chest recorded ECG amplitude (and <0.04 μV of at-scalp electrodes), providing a low-CFA window within which cortical activity may be measured without distortion from electrical discharges originating from the myocardium. After previous research (23), we selected a 140-ms epoch that occurred after the ECG T-wave (455–595 ms after R wave; Fig. 2). Physiological measures were then used as explanatory variables of changes in scalp-recorded HEPs at each point in the scalp, using an SPM instantiation of the general linear model (SPM5; www.fil.ion.ucl.ac.uk). This analysis entails interpolating the channel responses into a 2D image of scalp responses and forming statistical parametric maps of the T statistic in the usual way. We created SPMs testing for a main effect of stress and of parametric variation in the physiological measures. Changes in systolic blood pressure and neck-recorded ECG were included in design matrices assessing relationship with cardiac output and Hill parameter, respectively, such that only independent effects were reported. In SPM5, corrections for multiple comparisons over the scalp use a random field theory adjustment to the P values to control family-wise error. Because our data were smooth over the scalp, we chose to use P values based on the spatial extent of regions whose uncorrected P values exceeded 0.002. Suprathreshold data are also used for graphical display of significant regions (after projecting on to a scalp surface in 3D). Because of missing data, a separate model of the Hill parameter was used for a subset of patients. Associations between medication status and HEP effects were thoroughly tested. Left temporal HEP amplitude was reduced within patients prescribed beta blockers (either Atenolol or Bisoprolol). The significant associations between HEPs and both cardiac output and Hill parameter remained significant after controlling for beta-blocker status.
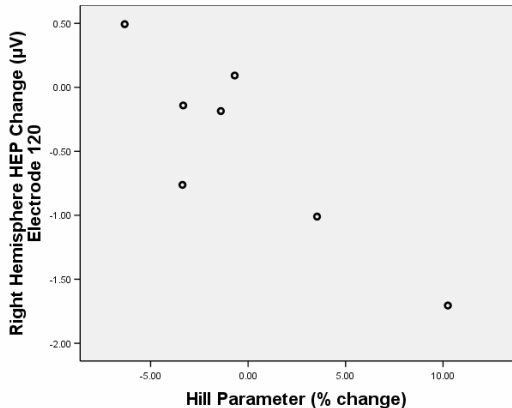
1. Lane R-D, Laukes C, Marcus F-I, Chesney M-A, Sechrest L, Gear K, Fortm C-L, Priori S-G, Schwartz P-J, Steptoe A (2005) *Psychosom Med* 67:359–365.
2. Lampert R, Shusterman V, Burg M-M, Lee F-A, Earley C, Goldberg A, McPherson C-A, Batsford W-P, Soufer R (2005) *J Cardiovasc Electrophysiol* 16:372–377.
3. Fries R, Konig J, Schafers H-J, Bohm M (2002) *Clin Cardiol* 25:474–478.
4. Oppenheimer S-M, Cechetto D-F, Hachinski V-C (1990) *Arch Neurol* 47:513–519.
5. Taggart P, Sutton P, Redfern C, Batchvarov V-N, Hnatkova K, Malik M, James U, Joseph A (2005) *Psychosom Med* 67:376–383.
6. Critchley H-D, Taggart P, Sutton P-M, Holdright D-R, Batchvarov V, Hnatkova K, Malik M, Dolan RJ (2005) *Brain* 128:75–85.
7. Nei M, Ho R-T, Abou-Khalil B-W, Drislane F-W, Liporace J (2004) *Epilepsia* 45:338–345.
8. Giannattasio C, Cattaneo B-M, Seravalle G, Grassi G, Mancia G (1991) *J Hypertens Suppl* 9:S43–S50.
9. Craig AD (2002) *Nat Rev Neurosci* 3:655–666.
10. Schwartz P-J, Vanoli E, Stramba-Badiale M, DeFerrari G-M, Billman G-E, Foreman RD (1988) *Circulation* 78:969–979.
11. Schwartz P-J (1999) *Eur Heart J* 1(Suppl H):H33–H43.
12. Rosen S-D, Paulesu E, Nihoyannopoulos P, Tousoulis D, Frackowiak, R-S (1996) *Ann Intern Med* 124:939–949.
13. Critchley H-D, Corfield D-R, Chandler M-P, Mathias C-J, Dolan R-J (2000) *J Physiol (London)* 523 (Pt 1):259–270.
14. Critchley H-D (2005) *J Comp Neurol* 493:154–166.
15. Harper R-M, Macey P-M, Woo M-A, Macey K-E, Keens T-G, Gozal D, Alger JR (2005) *J Neurophysiol* 93:1647–1658.
16. Kimmerly D-S, O'Leary D-D, Menon R-S, Gati J-S, Shoemaker J-K (2005) *J Physiol (London)* 569:331–345.
17. Schandry R, Sparrer B, Weitkunat R (1986) *Int J Neurosci* 22:261–275.
18. Montoya P, Schandry R, Muller A (1993) *Electroencephalogr Clin Neurophysiol* 88:163–172.
19. Pollatos O, Kirsch W, Schandry R (2005) *Brain Res Cogn* 25:948–962.
20. Pollatos O, Kirsch W, Schandry R (2005) *Hum Brain Mapp* 26:54–64.
21. Riordan H, Squires N-K, Brenner J (1990) *Psychophysiology* 27:559.
22. Schandry R, Montoya P (1996) *Biol Psychol* 42:75–85.
23. Dirlich G, Dietl T, Vogl L, Strian F (1998) *Electroencephalogr Clin Neurophysiol* 108:299–305.
24. Cervero F, Foreman R-D (1990) in *Central Regulation of Autonomic Functions*, eds Loewy AD, Spyer KM (Oxford Univ Press, Oxford), pp 104–125.
25. Reed S-D, Harver A, Katkin E-S (1990) in *Principles of Psychophysiology. Physical, Social, and Inferential Elements*, eds Cacioppo JT, Tassinary LG (Cambridge Univ Press, Cambridge, UK).
26. Kohl P, Ravens U (2003) *Prog Biophys Mol Biol* 82:3–9.
27. Henderson L-A, Richard C-A, Macey P-M, Runquist M-L, Yu P-L, Galons J-P, Harper R-M (2004) *J Appl Physiol* 96:693–703.
28. Zhang Z-H, Dougherty P-M, Oppenheimer S-M (1998) *Brain Res* 796:303–306.
29. Pollatos O, Schandry R (2004) *Psychophysiology* 41:476–482.
30. Angell James J-E (1971) *J Physiol (London)* 214:89–103.
31. Angell James J-E (1971) *J Physiol (London)* 213:42P–43P.
32. Wallin B-G (2006) *Clin Auton Res* 16:262–269.
33. Charkoudian N, Joyner M-J, Johnson C-P, Eisenach J, Dietz N, Wallin BG (2005) *J Physiol (London)* 568:315–321.
34. Oppenheimer S-M, Kulshreshtha N, Lenz F-A, Zhang Z, Rowland L-H (1998) *Clin Auton Res* 8:173–179.
35. Saleh T-M, Bauce L-G, Pittman Q-J (1997) *Am J Physiol* 272:R1631–R640.
36. Smith J-K, Barron K-W (1989) *Am J Physiol* 257:H1994–H2000.
37. Craig A-D (2003) *Curr Opin Neurobiol* 13:500–505.
38. Craig A-D (2005) *Trends Cognit Sci* 9:566–571.
39. Brooks J-C, Zambreanu L, Godinez A, Craig AD, Tracey I (2005) *NeuroImage* 27:201–209.
40. Critchley H-D, Wiens S, Rotshtein P, Ohman A, Dolan R (2004) *Nat Neurosci* 7:189–195.
41. Critchley H-D, Melmed R-N, Featherstone E, Mathias C-J, Dolan R-J (2002) *NeuroImage* 16:909–919.
42. Chandler M-J, Zhang J, Foreman R-D (1998) *J Neurophysiol* 80:628–637.
43. Damasio A (2003) *Ann NY Acad Sci* 1001:253–261.
44. Saper C-B (2002) *Annu Rev Neurosci* 25:433–469.
45. Oppenheimer S-M, Cechetto DF (1990) *Brain Res* 533:66–72.
46. Rosen S-D, Paulesu E, Wise R-J, Camici P-G (2002) *Heart* 87:513–519.
47. Augustine J-R (1996) *Brain Res Rev* 22:229–244.
48. Zhang Z-H, Dougherty P-M, Oppenheimer S-M (1999) *Neuroscience* 94:351–360.
49. Oppenheimer S-M, Cechetto D-F (1990) *Brain Res* 533:66–72.
50. Oppenheimer S-M (1993) *Stroke* 24(Suppl 12):I3–I5.
51. Lanza G-A, Crea F (2002) *Heart* 88:328–330.
52. Oppenheimer SM, Wilson JX, Guiraudon C, Cechetto DF (1991) *Brain Res* 550:115–121.
53. Williamson JW, McColl R, Mathews D (2003) *J Appl Physiol* 94:1726–1734.
54. Oppenheimer SM, Gelb A, Girvin JP, Hachinski VC (1992) *Neurology* 42:1727–1732.
55. Salo LM, Campos RR, McAllen RM (2006) *Clin Exp Pharmacol Physiol* 33:1255–1258.
56. Fagius J, Wallin BG (1980) *J Neurol Sci* 47:433–448.
57. Taggart P, Sutton P, Chalabi Z, Boyett M-R, Simon R, Elliott D, Gill J-S (2003) *Circulation* 107:285–289.
58. Delorme A, Makeig S (2004) *J Neurosci Methods* 134:9–21.
59. Merri M, Benhorin J, Alberti M, Locati E, Moss A-J (1998) *Circulation* 80:1301–1308.
60. Moss A-J (2005) *J Cardiovasc Electrophysiol* 16:952–953.

NEUROSCIENCE

HEP and Cardiac Output association by hemisphere

Left Hemisphere
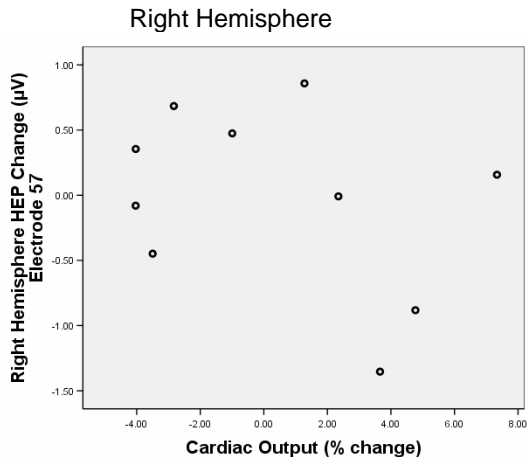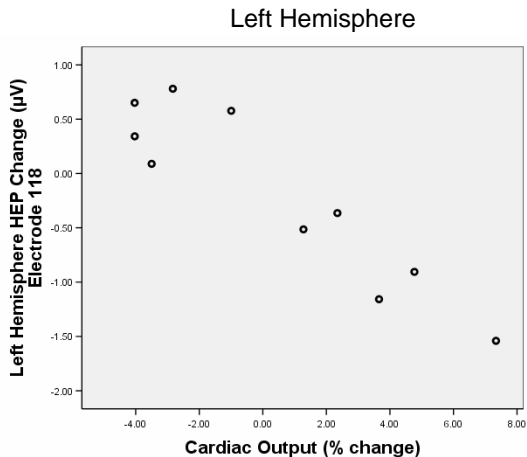
Right Hemisphere

HEP and Hill Parameter association by hemisphere

Left Hemisphere

Right Hemisphere